Homeopathy (2016) 105, 160–172

http://dx.doi.org/10.1016/j.homp.2015.09.006, available online at http://www.sciencedirect.com

ORIGINAL PAPER

Establishing the interfacial nano-structure and elemental composition of homeopathic medicines based on inorganic salts: a scientific approach

Mayur Kiran Temgire[1], Akkihebbal Krishnamurthy Suresh[1,2], Shantaram Govind Kane[1,*] and Jayesh Ramesh Bellare[1,2,*]

[1]*Department of Chemical Engineering, Indian Institute of Technology (IIT) Bombay, Adi Shankaracharya Marg, Powai, Mumbai 400076, Maharashtra, India*
[2]*Department of Biosciences and Bioengineering, Indian Institute of Technology (IIT) Bombay, Adi Shankaracharya Marg, Powai, Mumbai 400076, Maharashtra, India*

Extremely dilute systems arise in homeopathy, which uses dilution factors 10^{60}, 10^{400} and also higher. These amounts to potencies of 30c, 200c or more, those are far beyond Avogadro's number. There is extreme skepticism among scientists about the possibility of presence of starting materials due to these high dilutions. This has led modern scientists to believe homeopathy may be at its best a placebo effect. However, our recent studies on 30c and 200c metal based homeopathic medicines clearly revealed the presence of nanoparticles of starting metals, which were found to be retained due to the manufacturing processes involved, as published earlier.[9,10] Here, we use HR-TEM and STEM techniques to study medicines arising from inorganic salts as starting materials. We show that the inorganic starting materials are present as nano-scale particles in the medicines even at 1 M potency (having a large dilution factor of 10^{2000}). Thus this study has extended our physicochemical studies of metal based medicines to inorganic based medicines, and also to higher dilution. Further, we show that the particles develop a coat of silica: these particles were seen embedded in a meso-microporous silicate layer through interfacial encapsulation. Similar silicate coatings were also seen in metal based medicines. Thus, metal and inorganic salt based homeopathic medicines retain the starting material as nanoparticles encapsulated within a silicate coating. On the basis of these studies, we propose a universal microstructural hypothesis that all types of homeopathic medicines consist of silicate coated nano-structures dispersed in the solvent. *Homeopathy* (2016) **105**, 160–172.

Keywords: Homeopathy; Nanoparticles; Silicate coating; HR-Transmission electron microscopy

Introduction

Homeopathic medicines have dilution factors 10^{60}, 10^{400} and 10^{2000}, which amounts to 30c, 200c and 1 M potency are routinely used for treatment. These super Avogadro dilutions, if ideally done, should result in complete absence of a single molecule in a typical medicinal sample. To explain why activity is still retained, theories such as liquid memory,[1–4] clathrate formation,[5] and quantum physical[6,7] have been proposed in the past. Out of all theories only the silica hypothesis[8] implies the

*Correspondence: Jayesh Ramesh Bellare, Shantaram Govind Kane, Department of Chemical Engineering, Indian Institute of Technology (IIT) Bombay, Adi Shankaracharya Marg, Powai, Mumbai 400076, Maharashtra, India.
E-mail: mayurkt@iitb.ac.in, aksuresh@iitb.ac.in, sgkane@gmail.com, jb@iitb.ac.in
Received 18 August 2014; revised 8 May 2015; accepted 21 September 2015

presence of physical entities. In several industrial and biological processes we come across the ultra-high dilutions, but are not well studied since there are still no easy instrumental means to analyze the presence of trace materials. In the case of Homeopathic medicines the process of manufacture uses dilutions that exceed Avogadro's number by several orders of magnitude—so much so that one would not expect any measurable remnant of the starting material to be present. A scientific approach is necessary to fully understand the process of extreme dilutions and its implications to the materials involved from a physical and chemical viewpoint. Also important is the need to justify the prescribed process of manufacture consisting of the tedious task of arriving at ultra-high dilution involved in homeopathic medicine preparations, and relate it to the structure and function of the medicines.

There are few scientifically accepted studies in this area. The first is by Chikramane *et al.*[9] who have examined metal based homeopathic medicines and have shown that respective starting materials are still present as nanoparticles even at 200c potency. They have also explained this as a result of froth floatation[10] due to extensive foaming during succussion. The second is by Ives *et al.* (Anick and Ives,[8] Ives *et al.*[31]) who hypothesize but not prove that silica particles are present in the sample.

Silicates from the glass walls are continuously leaching out. We show that this silicate plays a key role in coating and retaining the starting materials in the solution. The role of this silicate shell is twofold, since it not only provides greatly enhanced colloidal stability in water, but also can be used to control the distance between core particles within assemblies through shell thickness.[11–25] From this point of view, extensive studies on metal–silica core–shell particles prepared by a liquid phase procedure have been made.[11, 12, 16, 17, 26]

In this present study, we have investigated the inorganic salt based homeopathic medicines such as Natrum muriaticum (NaCl), Kali muriaticum (KCl), Calcarea sulfuricum ($CaSO_4$), Natrum sulfuricum (Na_2SO_4) to show that these salts also remain in detectable quantities in the high potency medicines despite super Avogadro dilutions. Moreover, they are embedded in a silica layer containing nano-voids or air-bubbles. We further show similar findings for metal based medicines by reexamining the gold one in detailed and explain why the silica coating was not seen in our earlier work.

Materials and method

Materials

Five homeopathic medicines (6c, 30c, 200c and 1 M dilutions) Sodium chloride (*Natrum muriaticum or Natrum mur.*), Potassium Chloride (*Kali muriaticum or Kali mur.*), Calcium sulfate (*Calcarea Sulphurica or Calcarea sulph.*), Sodium sulfate (*Natrum sulphuricum or Natrum sulph.*), and Gold metal (*Aurum metallicum*) used in this study were purchased commercially from authorized distributors of a reputed homeopathic manufacturer in India (SBL), an Indian subsidiary of a multi-national firm viz. Wilmar Schwabe India Pvt. Ltd., and Healwell, Sintex Int. Ltd. The pure ethanol of HPLC grade was procured from Commercial Alcohols Inc., Canada. The formvar-carbon coated copper grids of 200 mesh were bought from Pacific Grid-Tech (U.S.A.). The manufacturing process used was ascertained by personal discussion with the manufacturers. It consisted of solid substances for Natrum mur, Kali mur, Natrum Sulph that were used as raw materials. 90 or 91% alcohol solutions were used in potentization along with lactose trituration for the process of dilutions. The dilutions were carried out by Hahnemannian method. Glass bottles used by the manufacturers for succussion were made of neutral glass or USP type III soda lime glass.

Method

Preparation of TEM grids: High Resolution TEM/EDX/STEM: Characterization of ultra-high dilute medicines was carried out using JEOL JEM 2100 electron microscope operated at 200 kV. HR-TEM formvar-carbon coated copper grids were held using anti-capillary forceps. A drop of medicine was directly placed on the grid. The drop was allowed to evaporate until it visually appeared to be dry, which took approximately ½ to 1 h in air at 23°C depending on the ambient humidity levels. After complete drying, another drop was placed as previously on the grid. This process was repeated 5–6 times. After letting the sample dry in air completely the grid was warmed using an IR lamp for about 15 min for ensuring a completely dry sample and removal of all solvent from the grid. During TEM, bright field and dark field images of the sample particles were captured with Orius 200 bottom mount camera. Selected area diffraction patterns were also taken. Energy dispersive X-ray analysis (EDX) was done with Oxford instruments (Model: EDS7688) for elemental analysis. Along with it STEM mapping was used for detailed distribution of elements present in the sample.

Typical TEM characterization: The most significant finding we had with TEM was the detection and imaging of inorganic salt based medicines, a typical figure of which is in Figure 1 (A–C), which shows a particle in bright field image along with selected area diffraction pattern of single crystal and energy dispersive X-ray analysis showing presence of active ingredients in Natrum mur. at 200c potency. The EDX shows prominent peaks of sodium and chlorine, together with other peaks of carbon, oxygen and copper, which are due to the substrate of Cu-grid coated with formvar-carbon.

Special precaution had to be taken to achieve all of the above: Inorganic salt based medicines were found to be electron beam sensitive and sublimed on exposure to the intense electron beam.[27] The phenomenon of sublimation can be observed in Figure 1 (D–L), where the salt particle is seen part by part disintegrating that begins from bottom of Figure 1(F) and continues to the top in

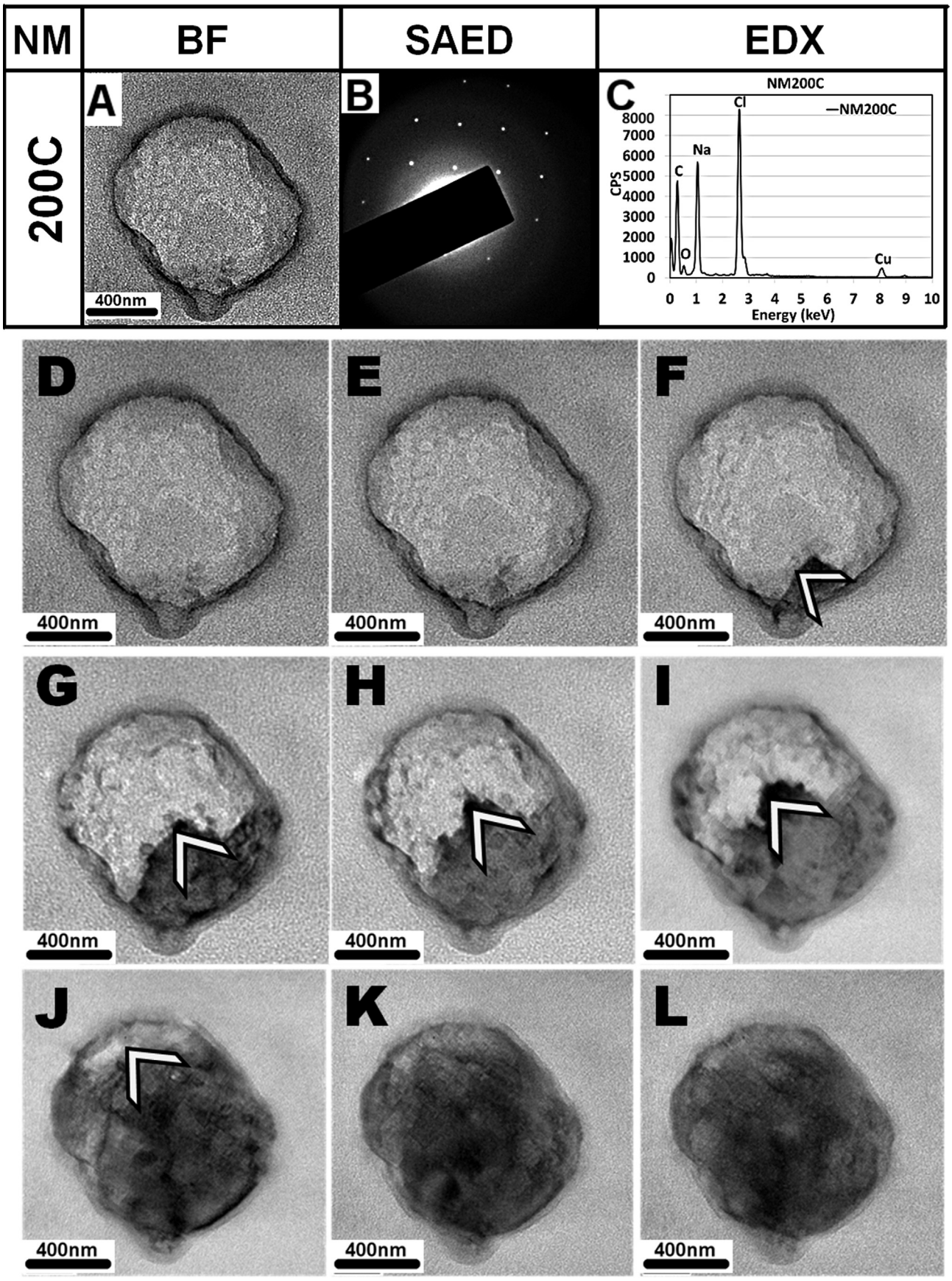

Figure 1 Transmission electron micrographs of Natrum muriaticum (NM 200c) showing (**A**) bright field image of sub-micron size particle, along with (**B**) Selected Area Electron Diffraction pattern and (**C**) Energy Dispersive X-ray analysis showing sodium and chlorine as prominent active elements present along with substrate carbon and a small oxygen peak. (**D**–**L**) are bright field images of a NaCl submicron particle subliming gradually, the subliming interface is marked with an arrow (**F**). The particle continues to sublime completely in successive micrographs till (**J**) in approximately 2 min leaving behind a dark black patch in the location of the particle.

Figure 1(J) indicated with an arrow leaving behind the depression in the region with high dark contrast. This makes it difficult to visualize the original microstructures of many particles due to sublimation. To reduce the time for observation, initially low magnification mode was used to find the area containing particles, then switching over to high magnification mode to focus on the particle. Sublimation rate was also cut down by reducing the spot size and thus decreasing the electron beam intensity. These two steps together enabled us to observe and photograph the structure of particles by preventing the sublimation. It enabled us to obtain elemental spectra and STEM mapping.

Sample particle size measurements and image processing were done by the help of Digital Micrograph – Gatan, Image-J and Gimp version 2.8 software.

Results and discussion

Establishing the presence of inorganic salts and elucidation of particle size and morphology by HR-TEM

In this study we have chosen four inorganic salts and one gold metal based homeopathic medicine. HR-TEM was used to obtain the particle size, morphology, bright field, dark field, selected area electron diffraction pattern (SAED) and energy dispersive X-ray analysis (EDX). Typical results of bright field, SAED and EDX are shown in Figure 1 and have been discussed above. The beam sensitive nature of samples is shown in Figure 1(D–L) and points to the need for careful microscopy. With these in mind, a systematic study was taken up. These are described for each medicine type below.

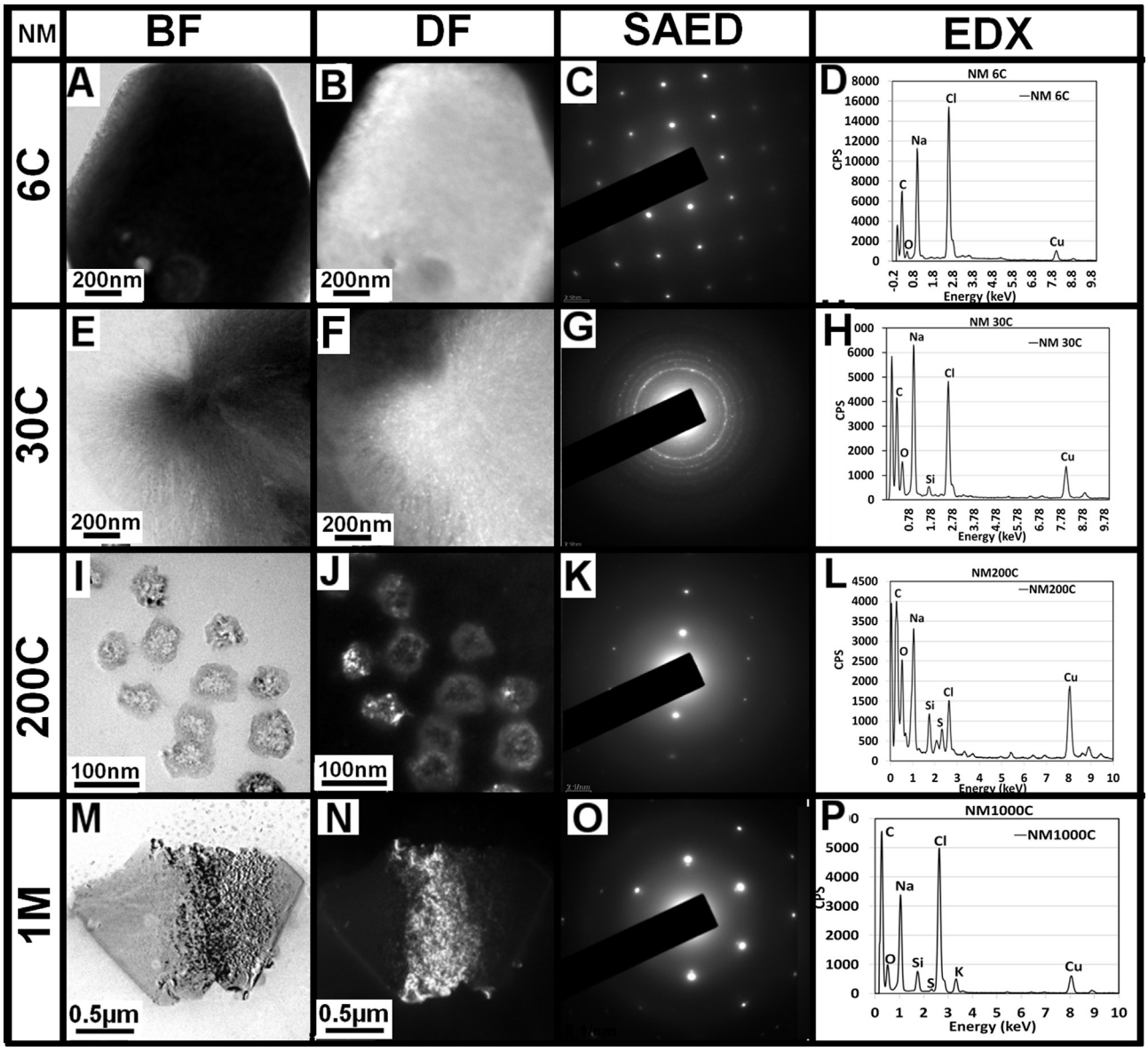

Figure 2 Natrum muriaticum 6c (A–D), 30c (E–H), 200c (I–L), 1 M (M–P) -SBL particles showing transmission electron microscopy in bright field (BF), dark field (DF), selected area electron diffraction patterns (SAED) modes and energy dispersive X-ray analysis having prominent peaks of sodium and chlorine followed by carbon, silicon and oxygen peaks, along with some minor sulfur and potassium peaks.

Natrum muriaticum (NaCl)

Figure 2 shows typical results on Natrum mur. homeopathic medicine with potencies of 6c, 30c, 200c, and 1 M. Bright field images of 6c, 30c and 1 M were of a single macro-particle, and in case of 200c there were many small nanoparticles seen. All the electron diffraction patterns are mosaic single crystal patterns in 6c, 200c, and 1 M, but 30c has polycrystalline pattern. EDX studies show significant peaks of sodium and chlorine in all potencies along with silica and oxygen peaks at higher potencies from 30c, 200c and 1 M. As we start with the low potency of 6c the EDX studies showed presence of active material sodium and chlorine dominant peaks. As we perform analysis of the higher potencies 30c, 200c and 1 M other elements also emerged were silica, oxygen, sulfur, potassium and oxygen. These supplementary elements are likely to have leached out from borosilicate glass. Other peaks of copper and carbon were due to the presence of copper grid and carbon coating. The elemental analysis suggests the presence of sodium silicates along with the active material.

Kali muriaticum (KCl)

Figure 3 shows typical results on Kali mur. homeopathic medicine with potencies from 6c, 30c, 200c, and 1 M. Bright field images of 6c, 30c, 200c and 1 M were single particles. Electron diffraction patterns in case of 6c and 1 M were polycrystalline, and 30c, and 200c were mosaic single crystal patterns. EDX studies showed significant peaks of sodium, silica and oxygen prominent peaks in all potencies along with potassium and chlorine peaks present. There is also a feeble sulfur peak presence seen in all potencies, which may have come from the color additives in amber glass bottles used in preparation of homeopathic

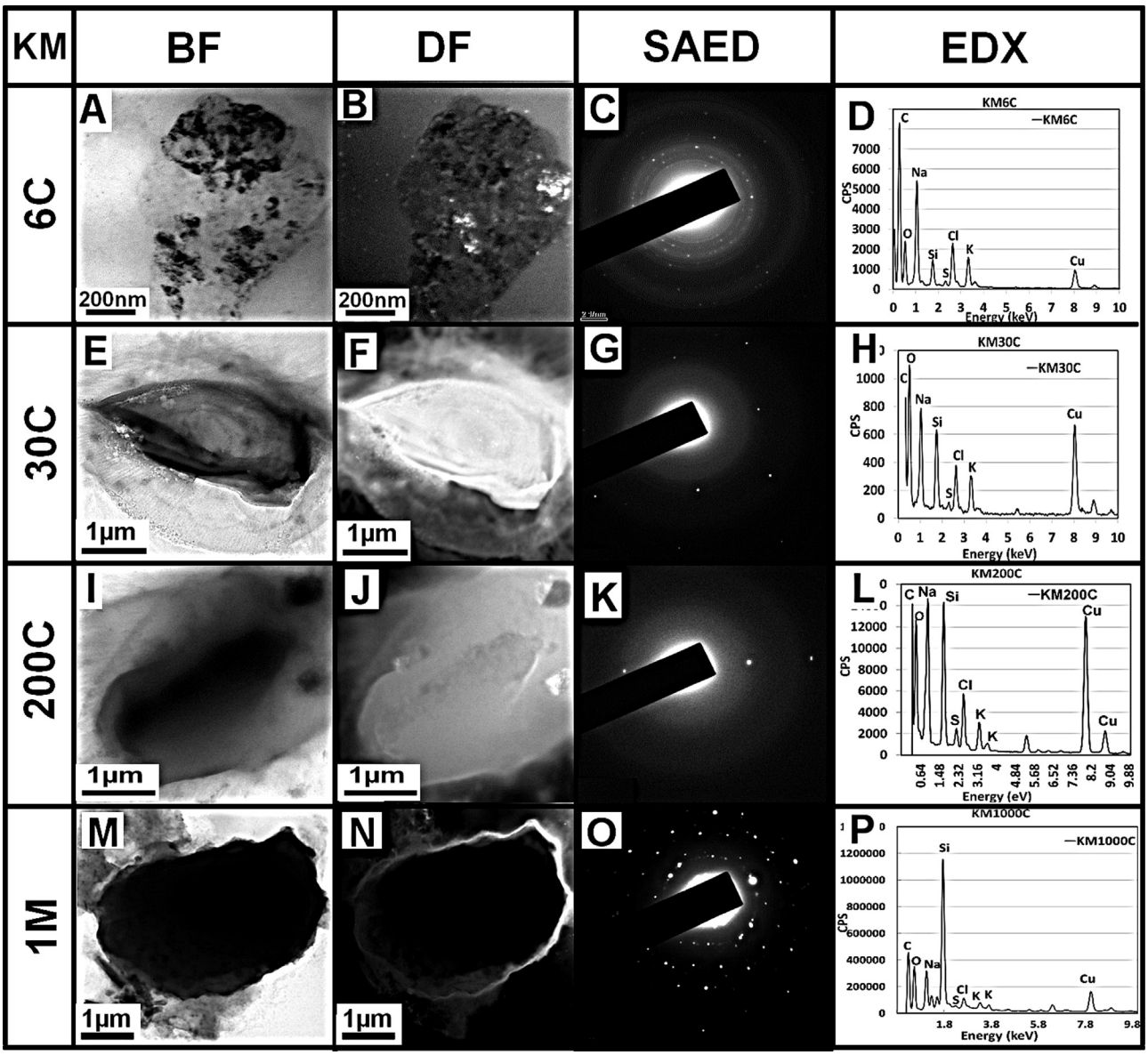

Figure 3 Kali muriaticum 6C (A–D), 30c (E–H), 200c (I–L), 1 M (M–P) -SBL micron size particles showing transmission electron microscopy in bright field (BF) images, dark field (DF) images, selected area electron diffraction pattern (SAED) modes and energy dispersive X-ray analysis (EDX) showing sodium, silicon and oxygen as prominent peaks along with potassium and chlorine peaks.

medicines. Here also, copper and carbon peaks were due to the substrate of copper grid with carbon coating.

Calcarea sulfurica ($CaSO_4$)

Figure 4 shows typical results of Calcarea sulfurica homeopathic medicine with potencies 6c, 30c, 200c, and 1 M. Bright field images in all the potencies show macro-clusters with varying contrast. Electron diffraction patterns in case of 6c and 1 M were polycrystalline, 30c, and 200c were mosaic single crystal patterns. EDX studies show significant peaks of sodium, silica, oxygen and calcium in all potencies. Sulfur and potassium peaks in all potencies have been damped. Remaining additional peaks of iron, copper and carbon were due to the presence of copper grid and carbon coating.

Natrum sulfuricum (Na_2SO_4)

Figure 5 shows typical results of Natrum sulfuricum homeopathic medicine with potencies 30c, 200c, and 1 M. Bright field images of 30c, 200c and 1 M are single macro-particles with varying contrast. Electron diffraction patterns in case of all potencies were mosaic single crystal patterns. An EDX study shows sodium, silica and oxygen prominent peaks in all potencies along with calcium and sulfur peaks present. As in all above medicines iron, copper and carbon peaks were due to the substrate of copper grid with carbon coating, and from the natural impurities in glass.

HR-TEM studies of Aurum metallicum

Fifth noble metal Aurum metallicum homeopathic medicine in Figure 6 shows results with bright field and dark field images of potency 30c is single macro-particle. The selected area electron diffraction shows polycrystalline pattern with annular spots. EDX studies show significant peaks of sodium, silica and oxygen. Gold peaks, though present, have been damped, since the fine gold particles were embedded in the large sodium silicate matrix. Gold

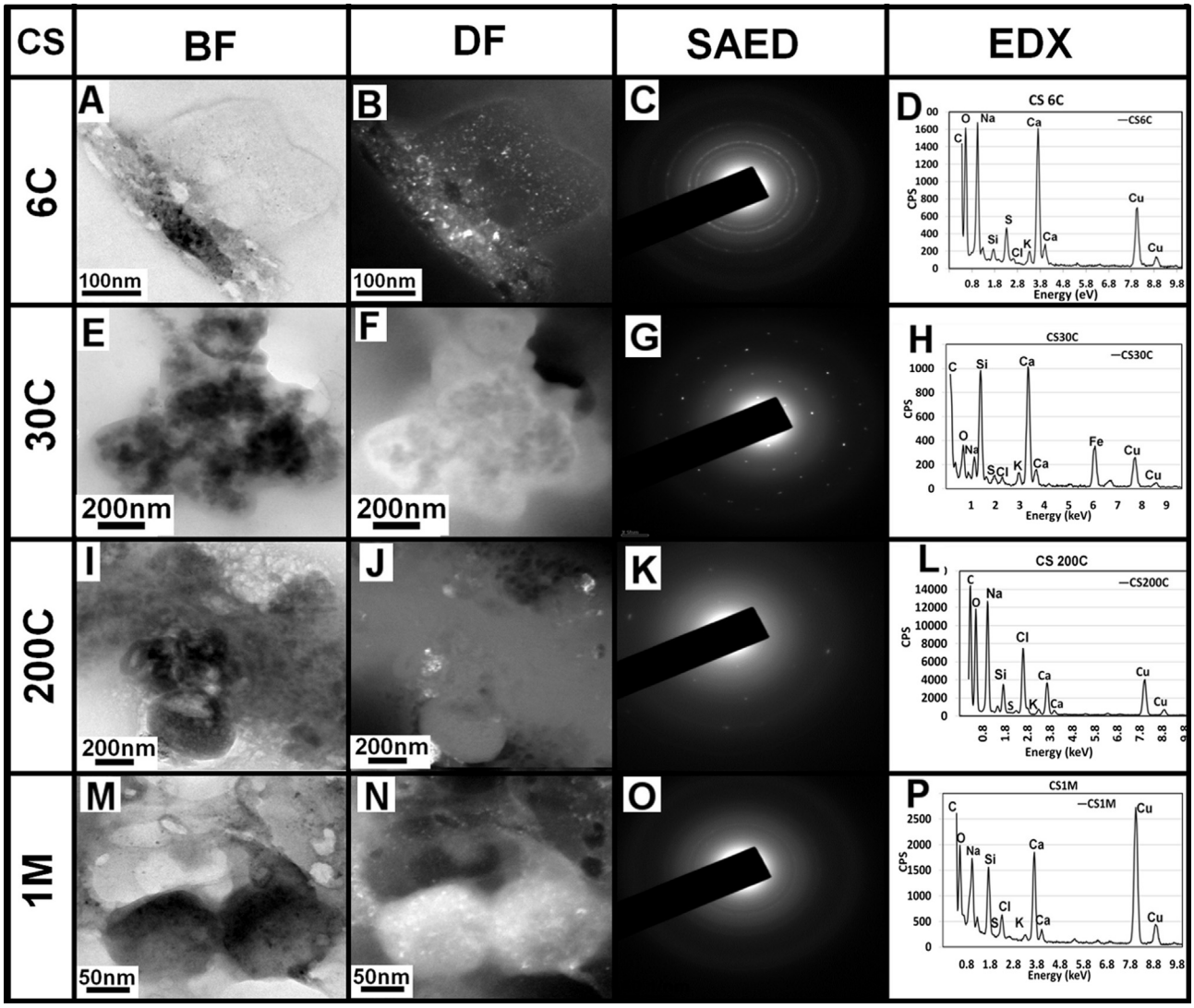

Figure 4 Calcarea sulfurica 6c (A–D), 30c (E–H), 200c (I–L), 1 M (M–P) -SIL particles showing TEM Bright field, Dark field, selected area electron diffraction pattern modes and energy dispersive X-ray analysis showing sodium, silicon, calcium and oxygen as prominent peaks along with sulfur, chlorine, and potassium as minor peaks. There are other additional peaks of copper, iron and carbon due to the carbon coated Cu-grids.

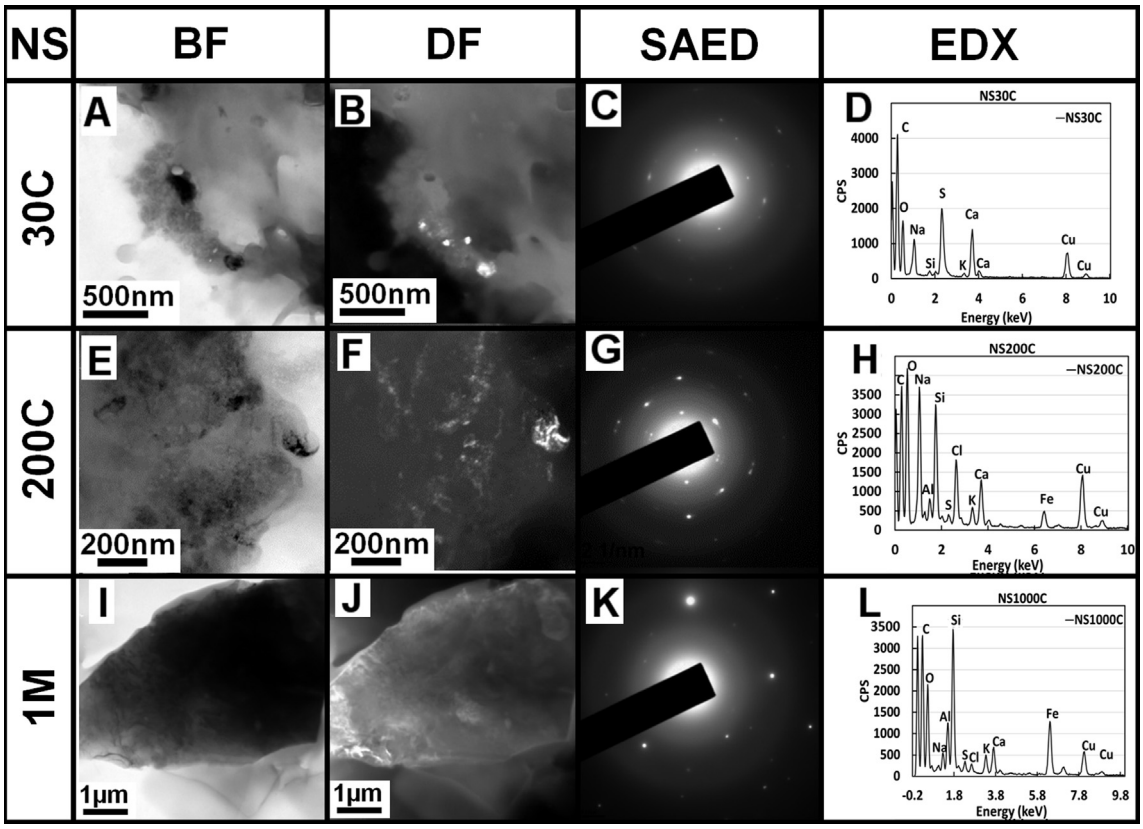

Figure 5 Natrum sulfuricum 6c (A–D), 30C (E–H), 200c (I–L), 1 M (M–P) -SBL particles showing TEM Bright field, Dark field, selected area electron diffraction pattern modes and energy dispersive X-ray analysis showing sodium, sulfur, silicon, chlorine, and oxygen as prominent peaks along with aluminum, calcium, and potassium.

was confirmed by indexing the diffraction pattern. Thus, coated nanoparticles of starting materials were commonly observed for both metal and inorganic salt based medicines.

In the earlier paper by Chikramane *et al.*[9] energy dispersive X-ray analysis was not available for elemental analysis so the overcoat may not have been detected. Moreover, the process of sublimation described above by us may have taken place to remove the coating because low-dose techniques were not used then.

Thus, in all four inorganic samples studied above, the starting elements Na, K, Ca, S were present in a particle along with Si and O. It is well known in the literature[8] that siloxanes leach out from glass walls and the amount of silicate leaching out from the glass wall has been estimated to be 3–5 ppm. Cations are also known to induce crystallization of siloxanes.[28] Taken together; it is highly likely that the inorganic salts are present in these particles along with silicates. We find that the inorganic particles in the final medicines arising from the starting materials get

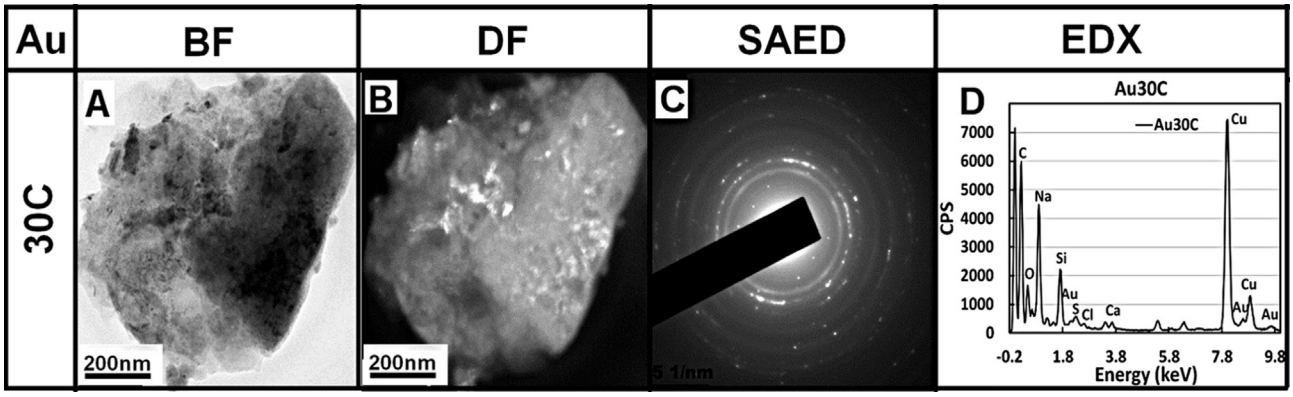

Figure 6 Aurum metallicum 30c (A–D) -SIL particles showing TEM Bright field, Dark field, selected area electron diffraction pattern (SAED) modes, and Energy Dispersive X-ray analysis showing sodium, silicon, and oxygen as prominent peaks along with gold, sulfur, calcium, and potassium. The presence of silicates is evident from the EDX.

coated with silicates during the manufacturing process as we shall show subsequently in this paper.

Particle morphology

Figure 7A, B shows core−shell morphology, consisting of inorganic salt core surrounded by sodium silicate. Both Natrum mur. 200c and Kali mur. 30c are seen to have coating of silicates. The size of all Natrum mur. nanoparticles range from 30 to 50 nm with a silicate coating of 10−20 nm, whereas Kali mur. is a present as a single large particle approximately 1.5 × 3.0 μm with a silicate coating of 0.5−1 μm. Also, seen in Figure 7(A) are two sodium chloride nanoparticles observed fusing into a single bigger nanoparticle with a common coating. We later explain the origin of the silicate coating during succussion. Since, the silicate polymer coat prevents the separation of these particles. SAED analysis of Figure 7(C) and (D) shows patterns consistent with both the inorganic salt and

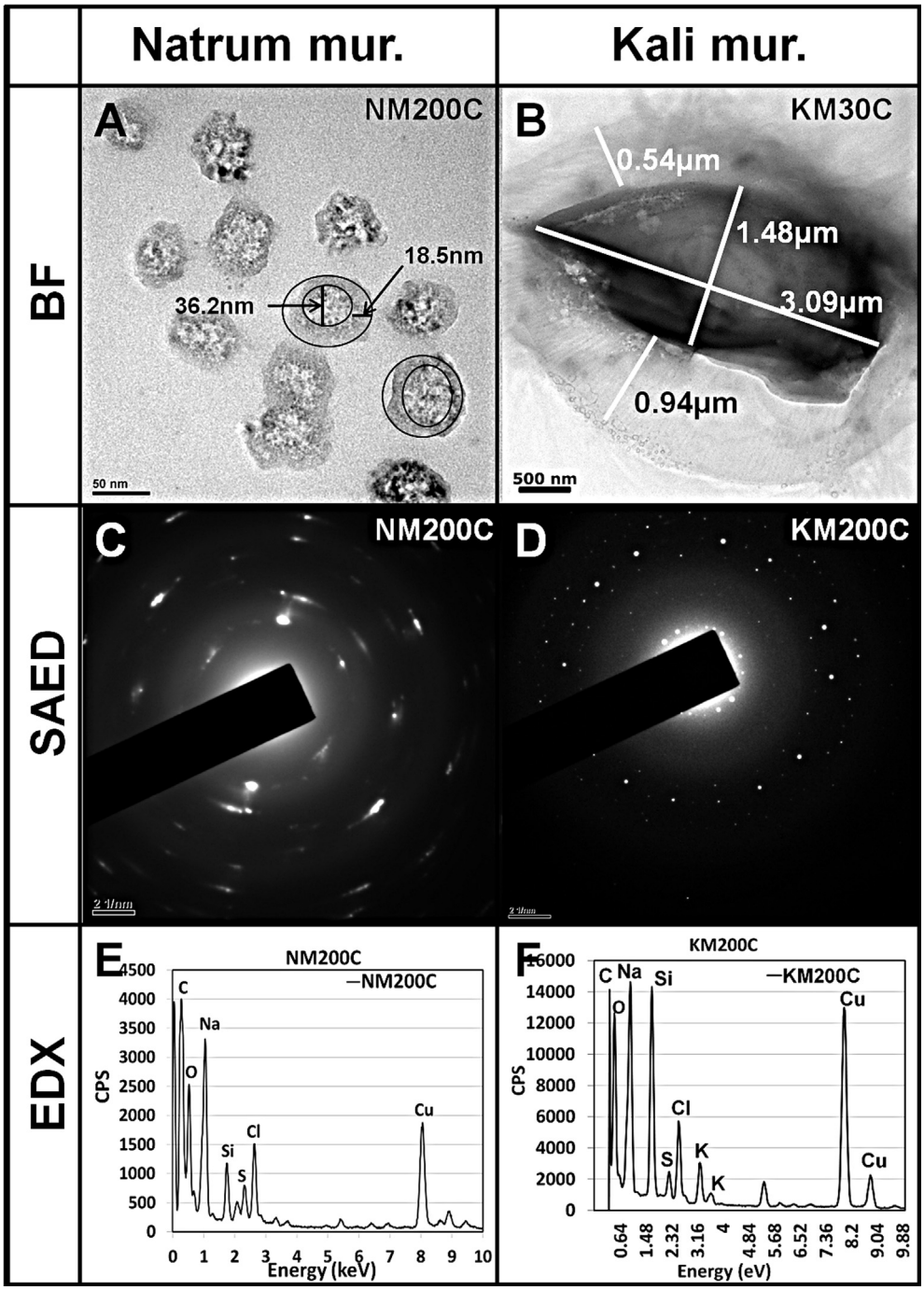

Figure 7 (A) Natrum muriaticum 200c nanosize particles, (B) Kali muriaticum 30c micron size particles, both coated with sodium silicate. (C) & (D) Selected area diffraction pattern of Natrum muriaticum 200c and Kali muriaticum 200c, (E) & (F) Energy dispersive X-ray analysis of Natrum muriaticum 200c and Kali muriaticum 200c showing presence of silicon, oxygen, and sulfur peaks along with other respective active elements sodium, potassium and chlorine peaks in them. Copper and carbon peaks were from the substrate copper grid that was coated with formvar-carbon. The presence of silicates is evident from the EDX, which is indexed as sodium silicate in Tables 1 and 2.

simultaneous presence of silicate in it. Natrum mur. 200c was indexed to sodium chloride and sodium silicate, whereas Kali mur. 200c was indexed to potassium chloride and sodium silicate, respectively.

Table 1 shows the d-spacings that were calculated from the diameters in the ring pattern of particles found in Natrum mur. 200c [Figure 7(C)]. These d-spacings match the strong lines from the standard JCPDS data for sodium chloride (std# 75-0306) and sodium silicate (std# 82-0604). Similarly, in case of Kali mur. 200c [Figure 7(D)] the d-spacing's were calculated from the diameter in the ring pattern. These d-spacings match well with the standard JCPDS data for potassium chloride (std# 77-2121) and sodium silicate (std# 82-0604). This confirms the presence of crystalline species of active elements along with the silicates in all the homeopathy medicines under study (as deduced from the SAED patterns) in spite the ultra-high dilutions in 30c, 200c and 1 M. Figure 7E showed presence of active material sodium and chlorine dominant peaks, along with oxygen, silicon, and sulfur peaks. Similarly, in Figure 7F the active ingredients potassium and chlorine peaks are present, along with sodium, silicon, oxygen, and sulfur peaks dominant. Other additional peaks of carbon and copper were from the substrate copper grid and formvar-carbon coating over it (Table 2).

Table 1 Selected area diffraction pattern of Natrum muriaticum 200c potency matching d-spacing for NaCl and $Na_2O.SiO_2$

NaCl			*$Na_2O.SiO_2$*			*NM200*
JCPDS-std#75-0306			*JCPDS-std#82-0604*			*Expt.*
h k l	*Rel-Int*	*d-spacing*	*h k l*	*Rel-Int*	*d-spacing*	*d-spacing*
		(Å)			*(Å)*	*(Å)*
			2 0 0	397	**5.233**	
			1 1 0	397	5.233	
1 1 1	94	3.2562	1 1 1	312	3.4983	
			3 1 0	999	**3.0197**	3.013
2 0 0	999	**2.82**	0 2 0	999	3.0197	2.836
			4 0 0	15	2.6165	
			2 2 0	15	2.6124	
			3 1 1	501	**2.5421**	2.545
			0 2 1	501	2.5421	
			0 0 2	561	2.355	
			2 0 2	4	2.1469	
			1 1 2	4	2.1469	
2 2 0	573	**1.994**	4 2 0	68	**1.9761**	1.913
			1 3 0	68	1.857	
			3 1 2	275	1.857	
			4 2 1	80	1.8205	
			1 3 1	80	1.8205	
			4 0 2	40	1.7504	
			2 2 2	40	1.7504	
3 1 1	17	1.7005	6 0 0	205	**1.7443**	1.747
2 2 2	162	**1.6281**	4 2 2	38	1.5137	1.632
4 0 0	64	**1.41**	3 3 2	204	**1.4002**	1.401
			2 4 1	10	1.3845	
3 3 1	7	1.2939	6 2 2	21	1.271	
4 2 0	152	**1.2611**	4 4 1	15	**1.2587**	1.23
4 2 2	102	1.1512				

Comparison of d-spacing for Natrum mur. 200c potency in Figure 8C electron diffraction pattern match NaCl and $Na_2O.SiO_2$ standard JCPDF # 75-0306 and 82-0604.
d-spacing values that are matching with the JCPDS std are represented in bold.

Trapping of nano-bubbles in meso-microporous sodium silicates

The silicate coated particles in Figure 8 clearly show meso-microporous channels available for entrapping nano-bubbles. In the literature it has been proposed that such channels may provide a way to load porous solids with high volume of gases.[22] It is also predicted that nano-bubbles are originated due to long-range attraction occurring in hydrophobic surfaces and reduce density.[24] In Figure 8(C) we were able to visualize entrapped nano-bubbles while coating of meso-microporous silicate cross-linked polymers. These trapped nano-bubbles (Figure 8(C)) in micropores vary from 5 to 50 nm in size. These may help to attach the particle to a bigger bubble that levitates the bigger silicate coated particles in solution by surpassing several drag and gravitational forces in the liquid and froth float to the air-liquid interface and get transferred to the next potency, as per the mechanism proposed by Chikramane *et al.*[10] Entrapment of these nano-bubbles was observed deep inside the micro-porous cavities too. There are several nano-bubbles present all around the coated particles. This levitation process carries with it several particles making the surface rich with coated active

Table 2 Selected area diffraction pattern of Kali muriaticum 200c potency matching d-spacing for KCl and $Na_2O.SiO_2$

KCl			*$Na_2O.SiO_2$*			*KM200C*
JCPDS-std#77-2121			*JCPDS-std#82-0604*			
h k l	*Rel-Int*	*d-spacing*	*h k l*	*Rel-Int*	*d-spacing*	*d-spacing*
		(Å)			*(Å)*	*(Å)*
			2 0 0	397	**5.233**	5.2024
			1 1 0	397	5.233	4.2989
1 0 0	4	3.67	1 1 1	312	**3.4983**	3.4591
			3 1 0	999	**3.0197**	3.0099
			0 2 0	999	3.0197	
1 1 0	999	**2.595**	4 0 0	15	**2.6165**	2.6095
			2 2 0	15	2.6124	
			3 1 1	501	**2.5421**	
			0 2 1	501	2.5421	2.4680
			0 0 2	561	2.355	
1 1 1	2	**2.1188**	2 0 2	4	**2.1469**	2.1551
			1 1 2	4	2.1469	
			4 2 0	68	1.9761	
			1 3 0	68	1.857	
			3 1 2	275	1.857	
			4 2 1	80	1.8205	
2 0 0	132	1.835	1 3 1	80	1.8205	
			4 0 2	40	**1.7504**	1.7285
			2 2 2	40	1.7504	
2 1 0	2	1.6412	6 0 0	205	**1.7443**	1.7065
			4 2 2	38	1.5137	
2 1 1	220	1.4982	3 3 2	204	1.4002	
			2 4 1	10	**1.3845**	1.3335
2 2 0	57	1.2975	6 2 2	21	1.271	
3 0 0	1	1.2233	4 4 1	15	1.2587	
3 1 0	72	1.1605				

Comparison of d-spacing for Kali mur. 200c potency in Figure 8D electron diffraction pattern match KCl and $Na_2O.SiO_2$ standard JCPDF # 77-2121 and 82-0604.

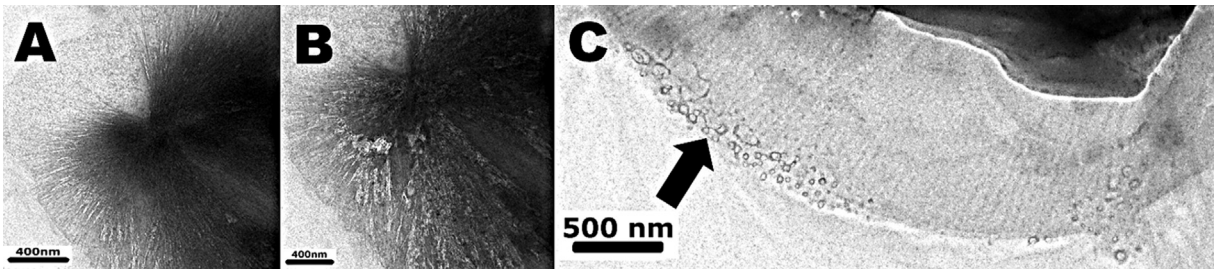

Figure 8 HR-Transmission electron microscopy bright field images of (A–B) Natrum muriaticum 30cshowing presence of meso-microporous structures of sodium silicate coated on sodium chloride and (C) Kali muriaticum 30c with nano-voids (air bubbles) have shown with arrow mark entrapped in meso-micropores.

particles. These images validate the mechanism predicted by Chikramane *et al.*[10] that due to rigorous turbulence in the headspace of glass bottle containing air gets entrapped in silicate polymer chains coating the starting materials. Due to succussion the liquid vortex is initiated at the surface and proceeds to the bottom of the glass bottle. Every succussion may generate new nanoparticles from the walls of the glass.

Elemental composition with STEM mapping

STEM mapping provides elemental distribution and mapping across the particles. This information is converted into a composite picture of the distribution of elements in the entire particle. Such maps are provided in Figure 9. Further confirmation of the elements location in the sample can be tracked by this image mapping technique. All the starting active element presence is observed in this method. Figure 9(a) has the elemental analysis for Natrum mur. 1 M which has Na, Cl, Si, and O. Sodium clusters match well with the chlorine clusters that are clearly seen with a mild presence of silicon and oxygen. Figure 9(b) shows the elements analyzed for Kali mur. 200c which shows presence of K, Cl, Na, Si, and O. Potassium small cluster match well with chlorine clusters along with clusters of sodium, silicon, and oxygen. Figure 9(c) is of Calcarea sulph. 1 M which has presence of Ca, S, Na, Si, and O elements that are dispersed throughout the dissociated particles spread evenly all over the particle region scanned.

Hypothesis for universal silica coating and retention

In view of the results obtained in the above study, we would like to propose a universal hypothesis of micro-mesoporous silica coat formation and retaining of the active ingredients in the core for all the classes of homeopathy based medicines. As soon as the sodium silicate, which has leached from the glass walls enters the ethanol solution it begins to polymerize into silicate chains.[29,30] Polymerization process (Figure 10) is initiated in presence of ethanol that acts as a crosslinking agent to the silicon in the sodium silicate solution. The cross-linked silicate chains initially forms a sticky gel-like mass that easily gets coated on to the nanoparticles of starting materials present in the solution. Later, these silicate polymer chains gain more elasto-plasticity and obtain a meso-microporous structure. This coating plays a key role in

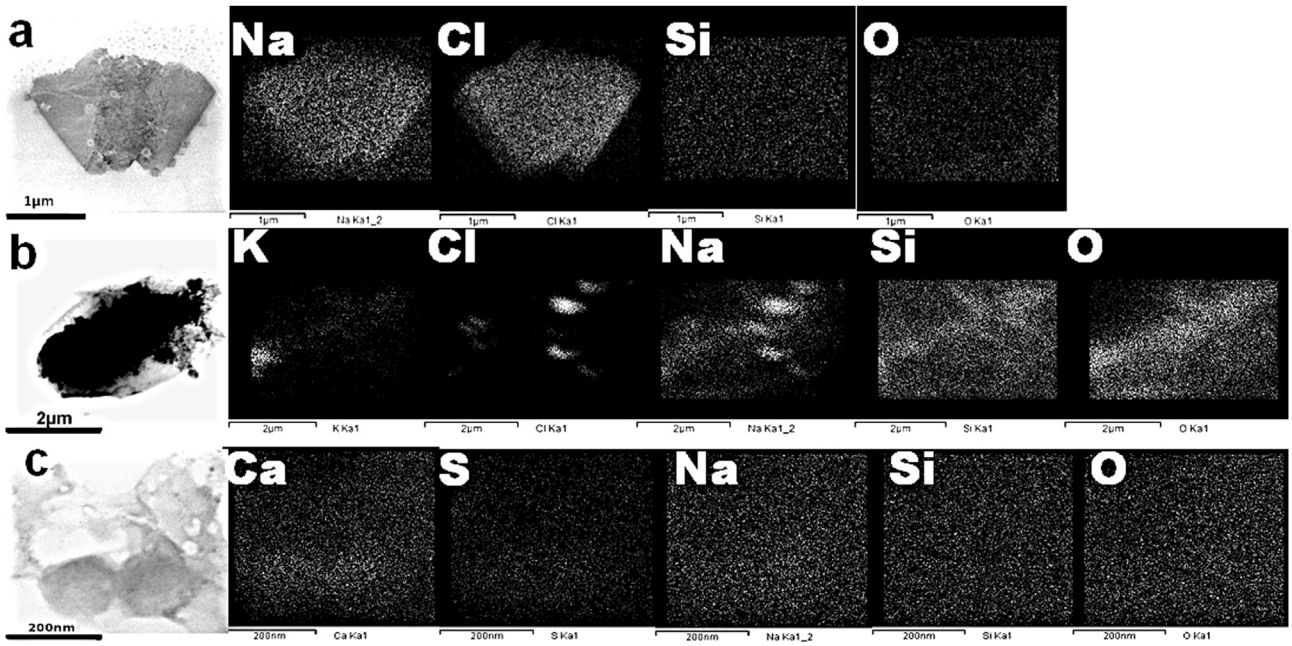

Figure 9 Scanning transmission electron microscopy elemental mapping images of (a) Natrum muriaticum 1 M, (b) Kali muriaticum 200C, and (c) Calcarea sulfurica 1 M showing the mapping of Na, K, Ca, S, Cl, Si, O elements.

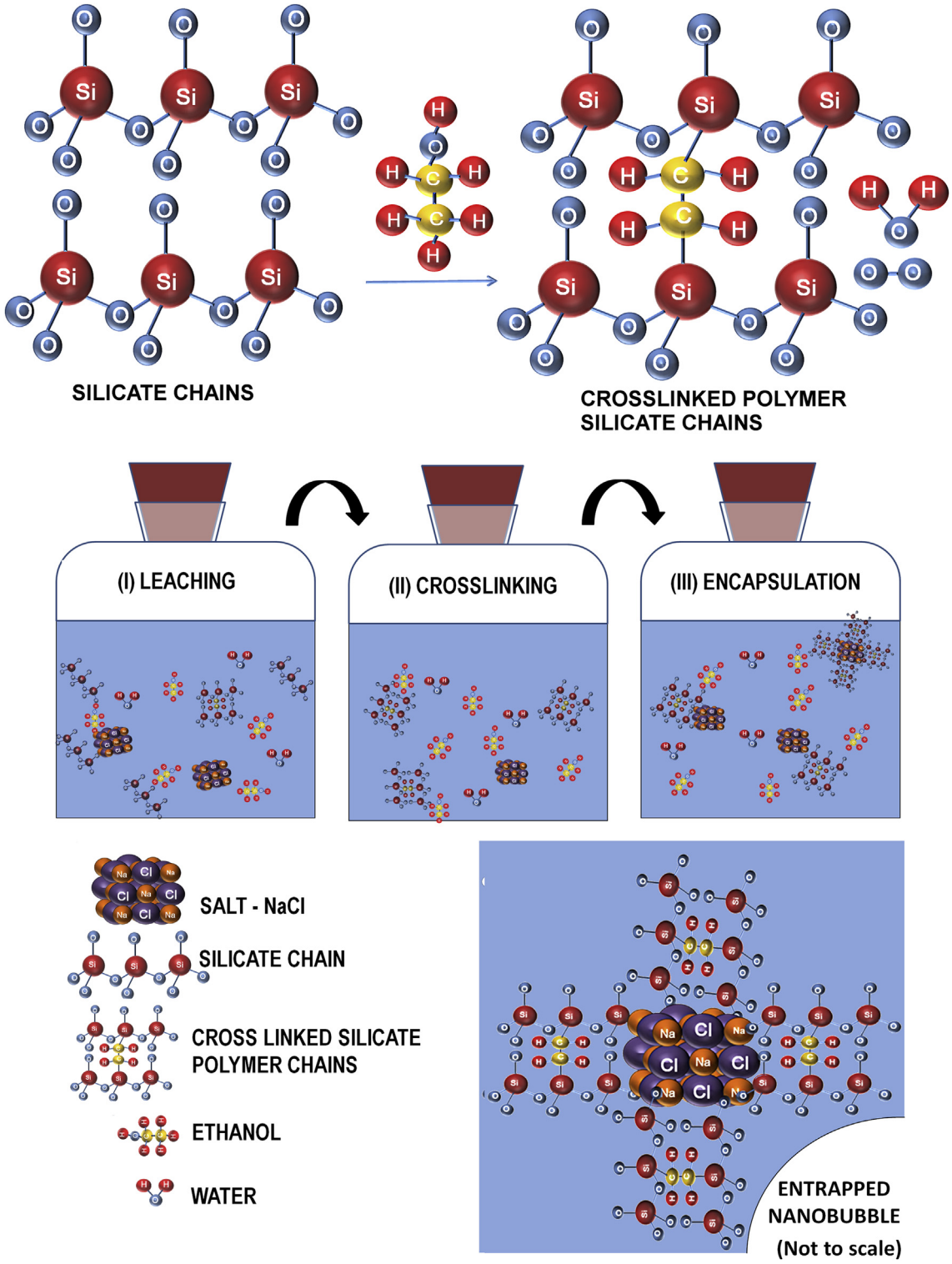

Figure 10 Schematic representation of silicate chains leached from glass walls during succussion process forming cross-linked silicate in presence of alcohol and preserving the starting ingredients by coating them. (I) initial leaching of silicate chains (II) intermediate crosslinking of silicate chains polymers. (III) Cross-linked silicate polymer chains coating active ingredient.

preventing dissolution of starting materials such as NaCl, KCl, etc in the solution.

Step 1: Formation of silicate coating and retention: Initially, lactose capping retains the active ingredients inside it during the grinding process. Subsequent succussion processes are responsible for dissolution of the lactose coating and enhancing the leaching out from the glass surface with release of more silicate chains in the ethanol solution. Succussion process also leads to excess leaching out of silica from the glass walls. It is known that the inorganic solutes also help in silicate formation.[8] Later these form long chains of silicates and initiate the polymerization in presence of ethanol. Smaller coated particles also come in vicinity of each other and fuse to form a bigger particle

with coating of silicate. These micro-mesoporous silicate nanoparticles serve as active ingredient in remedies as demonstrated by Ives *et al.*[31] This phenomenon was observed in Figure 7(A) of Natrum mur. 200c, in which two sodium chloride nanoparticles out of many are observed fusing into a single bigger nano-particle. Silicate chains in presence of alcohol cross-link to form polymer silicate chains seen in schematic representation of Figure 10. Further, the different stages from (I) Initial leaching of silicate from the glass walls, (II) Intermediate cross-linking of silicate polymer chains, and (III) Final stage of cross-linked polymer silicate chains coating the active ingredients and entrapping the nano-bubbles in them. As soon as the silica enters the solution, polymerization process is initiated by crosslinking of the silicate chains that adhere and coat firmly to the active nanoparticles due to their sticky gel like micro-mesoporous mass.

Step 2: Air-nanobubbles entrapment for nanoparticles levitation: The intense turbulence caused by the succussion process that effectively engulfs air from the headspace of the glass bottle. Meso-microporous coating of silicates entrap air nano-bubbles [Figure 7(C)] in the gap of cross-linked polymer silicate chains due to the vigorous shaking involved in succussion process. These air nano-bubbles later easily adhere to larger air bubbles and levitate the silicate coated active ingredient to the top surface and get transferred to the next potency. Entrapped air nano-bubbles formed during the repeated succussion thus participates proactively levitating the nanoparticles.

Thus the above steps result in a silica coat formation that retains the active ingredient along with the entrapment of nano-bubbles in micro-mesoporous silica. During succussion this leads to the levitation of nanoparticles that assists the whole process of capture, retention and transfer of the active ingredient to the next potency. Our findings establish the presence of silica, which is part of the hypothesis of Ives *et al.*[31] Based on the observations from the results of the above inorganic salts and gold metal based medicines we propose that this universal hypothesis applies not just for these but for all homeopathy based medicines.

We propose that no matter what starting material is present, it will be silica coated and the silica-coated particles will persist in higher potencies. The universality of this hypothesis needs to be proven for herbal and biological starting materials, and so far it is proven for metals and inorganic salts. Much more work is needed to address several uncertainties like quantitative measurement of species at these extreme dilutions and what, if anything, changes with potency. However, what becomes abundantly clear is that the material basis of these medicinal products is demonstrated for inorganic salt and metal based medicines. The medicinal and biological effects arising from these materials however remains to be proven at the low doses they are present.

Conclusion

Inorganic salt based homeopathic medicines retain particles, ranging from nano to large size particles, of the starting salt despite super Avogadro dilution. This is exactly analogous to the behavior of metal based homeopathic medicines. Furthermore, all the inorganic salt based homeopathic medicines studied here, and also the gold based medicine, show core−shell morphology consisting of the salt/metal at the core and a silicate shell arising from the glass wall, which provides an overcoat. Our understanding of the process of manufacture indicates that the silicate overcoat may also happen with all types of Homeopathic medicines including organics and nosodes, but that needs validation. Further, we have shown that the coating itself is micro-mesoporous and contains nano-voids and nano-bubbles presumably formed during the succussion process. The presence of such mesoporous coating in a wide range of homeopathic medicines agrees well, and gives credence to the froth floatation hypothesis. Thus, we now have a scientific explanation and microscopic evidence which explains why the particles containing starting materials are present even at extremely high potencies such as 1 M which correspond to dilutions of 1 part in 10^{2000}, well beyond what could be imagined heretofore.

Author contributions

The manuscript was written through contributions of all authors. All authors have given approval to the final version of the manuscript.

Funding sources

This work was supported primarily by a grant from Narotam Sekhsaria Foundation, and S Kane. Support in part came from Mrs. Sree Patel.

Conflicts of interest

The authors declare no competing financial interests.

Acknowledgment

This work was supported primarily by a grant from Narotam Sekhsaria Foundation (11DT001) and SG Kane. Support in part came from Mrs. Sree Patel. We acknowledge S Swaminarayan from Healwell and PN Varma from Schwabe India for providing technical details about the manufacturing process. We thank the Department of Science and Technology (DST), Government of India, for support through FIST, Nanomission (11DST019, & 11DST016), IRPHA and SERC schemes and IITB Central Facilities (13IRCCCF003) for CryoHR-TEM in Department of Chemical Engineering, IIT Bombay.

References

1 Davenas E, Beauvais F, Amara J, *et al*. Human basoph degranulation triggered by very dilute antiserum against IgE. *Nature* 1988; **333**: 816−818.
2 Chaplin MF. The memory of water: an overview. *Homeopathy* 2007; **96**: 143−150.

3 Teixeira J. Can water possibly have a memory? a sceptica view. *Homeopathy* 2007; **96**: 158−162.
4 Rao ML, Roy R, Bell IR, Hoover R. The defining role of structure (including epitaxy) in the plausibility of homeopathy. *Homeopathy* 2007; **96**: 175−182.
5 Anagnostatos GS. Small water clusters (Clathrates) in the homoeopathic preparation process. In: Endler PC, Schulte J (eds). *Ultra High Dilution – Physiology and Physics*. Dordrecht, The Netherlands: Kluwe Academic Publishers, 1994, pp 121−128.
6 Walach H, Jonas WB, Ives J, van Wijk R, Weingärtner O. Research on homeopathy: state of the art. *J Altern Complement Med* 2005; **11**: 813−829.
7 Davydov AS. Energy and electron transport in biological systems. In: Ho MW, Popp FA, Warnke U (eds). *Bioelectrodynamics and Biocommunication*. Singapore: World Scientific Publishing Co. Pte. Ltd, 1994, pp 411−430 [Chap. 17].
8 Anick DJ, Ives JA. The silica hypothesis for homeopathy: physical chemistry. *Homeopathy* 2007; **96**: 189−195.
9 Chikramane PS, Suresh AK, Bellare JR, Kane SG. Extreme homeopathic dilutions retain starting materials: a nanoparticulate perspective. *Homeopathy* 2010; **99**: 231−242.
10 Chikramane PS, Kalita D, Suresh AK, Kane SG, Bellare JR. Why extreme dilutions reach non-zero asymptotes: a nanoparticulate hypothesis based on froth flotation. *Langmuir* 2012; **13**(28): 15864−15875.
11 Liz-Marzán LM, Giersig M, Mulvaney P. Synthesis of nanosized gold-silica core-shell particles. *Langmuir* 1996; **12**: 4329−4335.
12 Ung T, Liz-Marzán LM, Mulvaney P. Controlled method for silica coating of silver colloids. influence of coating on the rate of chemical reactions. *Langmuir* 1998; **14**: 3740−3748.
13 Marinakos SM, Shultz DA, Feldheim DL. Gold nanoparticles as templates for the synthesis of hollow nanometer-sized conductive polymer capsules. *Adv Mater* 1999; **11**: 34−37.
14 Hardikar VV, Matijevic E. Coating of nanosize silver particles with silica. *J Colloid Interface Sci* 2000; **221**: 133−136.
15 Hall SR, Davis SA, Mann S. Condensation of organosilica hybrid shells on nanoparticle templates: a direct synthetic route to functionalized core−shell colloids. *Langmuir* 2000; **16**: 1454−1456.
16 Mulvaney P, Liz-Marzán LM, Giersig M, Ung T. Silica encapsulation of quantum dots and metal clusters. *J Mater Chem* 2000; **10**: 1259−1270.
17 Kobayashi Y, Correa-Duarte MA, Liz-Marzán LM. Sol−gel processing of silica-coated gold nanoparticles. *Langmuir* 2001; **17**: 6375−6379.
18 Cho G, Fung BM, Glatzhofer DT, Lee JS, Shul YG. Preparation and characterization of polypyrrole-coated nanosized novel ceramics. *Langmuir* 2001; **17**: 456−460.
19 Tago T, Hatsuta T, Nagase R, Kishida M, Wakabayashi K. *Kagaku Kogaku Ronbunshu* 2001; **27**: 288 [in Japanese].
20 Wang H, Nakamura H, Yao Y, Maeda H, Abe E. Effect of solvents on the preparation of silica-coated magnetic particles. *Chem Lett* 2001;1168−1169.
21 Lu Y, Yin Z, Li Z, Xia Y. Synthesis and self-assembly of Au@SiO2 core-shell colloids. *Nano Lett* 2002; **2**: 785−788.
22 Jana NR, Earhart C, Ying JY. Synthesis of water-soluble and functionalized nanoparticles by silica coating. *Chem Mater* 2007; **19**: 5074−5082.
23 Dimas D, Giannopaulou I, Panias D. Polymerization in sodium silicate solutions: a fundamental process in geopolymerization technology. *J Mat Sc* 2009; **44**: 3719−3730.
24 Attard P. The stability of nanobubbles. *Eur Phys J Sp Top* 2013;1−22.
25 Varma PN, Vaid I. In: *Encyclopedia of Homoeopathic Pharmacopoeia & Drug; Index B*. New Delhi: Jain Publishers, 2007, pp 2722−2745.
26 Joo SH, Park JY, Tsung CK, Yamada Y, Yang P, Somorjai GA. Thermally stable Pt/mesoporous silica core−shell nanocatalysts for high-temperature reactions. *Nat Mater* 2009; **8**: 126−131.
27 Egerton RF, Li P, Malac M. Radiation damage in the TEM and SEM. *Micron* 2004; **35**: 399−409.
28 Kinradet SD, Pole DL. Effect of alkali-metal cations on the chemistry of aqueous silicate solutions. *Inorg Chem* 1992; **31**: 4558−4563.
29 University of Maine, Lecture connections homepage, polymers: slime & superball http://interchemnet.um.maine.edu/newnav/Homepage/Highschool/Slime/lecpolymers2.htm [accessed January 3, 2014].
30 Gill I, Ballesteros A. Encapsulation of biologicals within silicate, siloxane, and hybrid sol-gel polymers: an efficient and generic approach. *J Am Chem Soc* 1998; **120**: 8587−8598.
31 Ives JA, Moffett JR, Peethambaran A, *et al*. Enzyme stabilization by glass-derived silicates in glass-exposed aqueous solutions. *Homeopathy* 2010; **99**: 15−24.